

Submitted to The Astrophysical Journal, January 1997

## Cusps and Triaxiality

David Merritt

Department of Physics and Astronomy, Rutgers University, New Brunswick, NJ 08855

### ABSTRACT

Statler (1987) demonstrated that self-consistent triaxial models with the perfect density law could be constructed for virtually any choice of axis ratios. His experiments are repeated here using triaxial mass models based on Jaffe's density law, which has a central density that diverges as  $r^{-2}$ , similar to what is observed in low-luminosity elliptical galaxies. Most of the boxlike orbits are found to be stochastic in these models. Because timescales for chaotic mixing are generally shorter than a galaxy lifetime in triaxial models with strong cusps, and because fully-mixed stochastic orbits have shapes that are poorly suited to reproducing a triaxial figure, only the regular orbits are included when searching for self-consistent solutions. As a result of the restriction to regular orbits, self-consistent solutions are found only for mass models with a modest range of shapes, either nearly oblate, nearly prolate or nearly spherical. This result may explain in part the narrow range of elliptical galaxy properties.

### 1. Introduction

The hypothesis that elliptical galaxies are generically triaxial in shape has been challenged from two directions in recent years. Observational evidence for triaxiality, which at one time seemed compelling, is now viewed with more skepticism. While isophotal twists are fairly common in early-type galaxies, many of these systems are probably barred S0's, not bona-fide ellipticals (Fasano & Bonoli 1989; Nieto et al. 1992). Kinematical tests for triaxiality, when applied to uniformly selected samples, suggest that few if any elliptical galaxies need be strongly triaxial in shape (Franx, Illingworth & de Zeeuw 1991). Detailed modelling of a few ellipticals with well-observed rotational velocity fields has mostly failed to reveal convincing evidence for triaxiality, at least in the central regions where the stellar distribution is likely to be relaxed (Statler 1994; Qian et al. 1995; Statler, Smecker-Hane & Cecil 1996). Although strong departures from axisymmetry are observed in a few bona-fide

elliptical galaxies, many of these have probably undergone tidal interactions or mergers in the recent past and hence are not in a steady state (e.g. NGC 1549, Longo et al. 1994; NGC 4589, Möllenhoff & Bender 1989; Centaurus A, Hui et al. 1995). And the discovery of lenticular systems with significant counterrotation (Rubin, Graham & Kenney 1992; Merrifield & Kuijen 1992) has weakened the conceptual link between velocity anisotropy and triaxiality.

On the theoretical side, a number of recent studies have emphasized the predominance of chaotic motion in the phase space of realistic triaxial potentials (Schwarzschild 1993; Merritt & Fridman 1996; Merritt & Valluri 1996; Papaphilippou & Laskar 1997). Most of the boxlike orbits in triaxial models with strong cusps, i.e. models in which the central density diverges more rapidly than  $\rho \propto r^{-1}$  at the center, are stochastic. Such cusps appear to be ubiquitous in low-luminosity ellipticals,  $M_V \gtrsim -20.5$  (Gebhardt et al. 1996). Furthermore, numerical experiments demonstrate that the chaos in triaxial models with high central densities can redistribute stars in phase space on timescales that are short compared to galaxy lifetimes (Merritt & Valluri 1996). The mechanism that drives this relaxation is chaotic mixing (Kandrup & Mahon 1994, 1995); in a fully-mixed system, the phase space density is constant throughout the stochastic parts of phase space at every energy. The loss of freedom that results from forcing the stochastic orbits to be fully mixed can preclude a self-consistent triaxial equilibrium (Merritt & Fridman 1996).

The goal of the present paper is to determine the degree to which triaxiality can be supported in galaxies with high central densities. The approach is similar to that of Statler (1987), who constructed self-consistent models of triaxial galaxies with the “perfect” density law, characterized by an unphysically large core. Orbit in the perfect ellipsoid are all regular and fall into one of just four families: the short-axis tubes; the inner- and outer long-axis tubes; and the boxes (Kuzmin 1973; de Zeeuw & Lynden-Bell 1985). Statler showed that linear superposition of orbits from the four families could reproduce the mass distribution of the perfect ellipsoid for virtually any choice of the axis ratios  $c/a$  and  $b/a$ . Furthermore he found that his solutions were highly nonunique, in the sense that stars could be apportioned in significantly different ways between the four families without violating self-consistency. However all of his solutions required significant numbers of stars to be assigned to box orbits. The importance of box orbits for the triaxial self-consistency problem was stressed also by Schwarzschild (1979, 1982) who constructed models based on the modified Hubble law. While orbits in the triaxial Hubble model are not all regular, Schwarzschild’s models contained only small numbers of stochastic orbits (Merritt 1980).

The absence of box orbits in triaxial models with realistic density profiles might be expected to limit the allowed degree of triaxiality. Schwarzschild (1993) found this to be

true in highly flattened, scale-free ( $\rho \propto r^{-2}$ ) triaxial models, and Merritt & Fridman (1996, hereafter Paper I) showed that a “maximally triaxial” model with Jaffe’s (1983) density law

$$\rho(m) = \rho_0 m^{-2} (1+m)^{-2}, \quad m^2 = \frac{x^2}{a^2} + \frac{y^2}{b^2} + \frac{z^2}{c^2} \quad (1)$$

and  $c/a = 0.5$  could not be reproduced using just the regular orbits.

Here, the numerical experiments of Paper I are extended to triaxial mass models with a range of axis ratios. Jaffe’s law (1) for the radial density profile is adopted throughout; thus these models are reasonable representations of elliptical galaxies fainter than  $M_V \approx -20.5$ , almost all of which are observed to contain central density cusps with logarithmic slopes  $\gamma$  close to 2 (Gebhardt et al. 1996). Brighter ellipticals,  $-22 \lesssim M_V \lesssim -20.5$ , also have power-law cusps but with a range of slopes,  $0 \lesssim \gamma \lesssim 2$ ; the brightest ellipticals,  $M_V \lesssim -22$ , tend to have the weakest cusps,  $\gamma \lesssim 1$  (Merritt & Fridman 1995). There is increasingly strong evidence for nuclear black holes containing  $\sim 1\%$  of the stellar mass in elliptical galaxies of all luminosities (Kormendy & Richstone 1995). Since the behavior of boxlike orbits in triaxial models with central singularities is similar to that of models with strong cusps (Merritt & Valluri 1996), the models studied here are likely to be relevant at some level to elliptical galaxies of all luminosities.

Libraries of orbits were computed in the potentials corresponding to these mass models, and linear superpositions of orbits were sought that yielded the mass of the model in a discrete grid of cells. Orbits were tested for stochasticity by computing their Liapunov exponents; as expected, most of the boxlike orbits were found to be stochastic. In a strictly time-independent model, stochastic orbits can be included only in the form of invariant ensembles, one per energy, that correspond to a uniform filling of chaotic phase space (Kandrup & Mahon 1994). Such ensembles are generally rounder than the model and not very useful for reconstructing the assumed mass distribution. Furthermore, in triaxial potentials with strong cusps, the chaotic mixing timescale over which stochastic phase space would be uniformly filled is generally shorter than a galaxy lifetime, particularly near the galaxy center (Merritt & Valluri 1996). Hence, in the current study, the stochastic orbits were simply deleted from the orbit libraries when searching for self-consistent solutions.

This limitation to regular orbits – mostly tubes, with some “boxlet” families – was found to impose severe restrictions on the shapes of self-consistent models. Strongly triaxial models, which would heavily weight the box orbits, are ruled out. Only nearly oblate, prolate or spherical models are allowed; such models require only a small contribution from non-tube orbits. These results suggest that the striking regularity in the observed properties of elliptical galaxies – the avoidance of strongly triaxial shapes, and the narrow range of kinematical behaviors – might be due in part to the restrictions imposed by chaos

on the population of phase space.

The algorithms used here to compute orbits, evaluate Liapunov exponents and construct self-consistent solutions were similar in most respects to those described in Paper I. Accordingly, only a brief discussion of the numerical methods is given here in §2. §3 presents the grid of 25 triaxial mass models and their orbital populations. The results from the self-consistent modelling are presented in §4. Implications for the structure of real elliptical galaxies are discussed in §5.

## 2. Numerical Methods

The grid of 25 mass models is displayed in Figure 1. The short-to-long axis ratio  $c/a$  was assigned a value from the set  $(0.4, 0.5, 0.6, 0.7, 0.8)$ , and the triaxiality parameter  $T = (a^2 - b^2)/(a^2 - c^2)$  was set equal to 0.1 (nearly oblate), 0.3, 0.5, 0.7, or 0.9 (nearly prolate).

For each mass model, 6840 orbits were integrated for 50 dynamical times  $T_D(E)$ , defined as the period of the 1:1 resonant orbit in the  $x - y$  plane at energy  $E$ . A 7/8 order Runge-Kutta algorithm with variable step size was used for the integrations. Initial conditions were assigned as in Paper I, from one of two grids of starting points: either on an equipotential surface with zero initial velocity (stationary), or in the  $x - z$  plane with  $v_x = v_z = 0$  ( $x - z$ ). Orbits started in the  $x - z$  plane are mostly tube orbits, while those started on an equipotential surface are boxlike, passing close to the center. Orbits with both sets of initial conditions were assigned one of a set of 20 energies, defined as the values of the potential on the  $x$ -axis of a set of ellipsoidal shells – with the same axis ratios as the density – that divide the model into 21 sections of equal mass. The grid of starting points at each energy is described in Paper I; it contained 150 orbits per shell in  $x - z$  initial condition space, and 192 orbits per shell in stationary initial condition space.

Stochasticity was detected by computing the largest Liapunov exponent  $\sigma_1$  for each orbit, defined as the average (over 50 dynamical times) of the exponential rate of divergence between the orbit and an infinitesimally-nearby orbit. At each energy and for each of the initial condition grids, a histogram of the  $\sigma_1$  values was constructed. These histograms invariably exhibited strong bimodality, with one narrow peak near zero (the regular orbits) and another, more diffuse peak centered around larger values of  $\sigma_1$  (the stochastic orbits). As in Paper I, this scheme might sometimes mistake stochastic orbits for regular orbits, since some stochastic orbits remain “trapped” near regular parts of phase space for long periods of time. However, any stochastic orbits that are mis-classified in this way are

effectively regular, since they can be counted on to mimic regular orbits for many dynamical times.

### 3. Orbit Families

Figure 2 gives the average number of stochastic orbits per shell in both initial-condition spaces for each of the 25 mass models. Typically only a few percent of the orbits from the  $x - z$  initial condition space were found to be stochastic, but the fraction of stochastic orbits from the stationary initial condition space was much larger, usually more than one-half. While the numbers in Figure 2 can not be simply translated into phase-space fractions, they suggest that stochasticity of the boxlike orbits is most important in strongly triaxial or nearly prolate mass models, and least important in nearly oblate models. (Of course, the boxlike orbits occupy only a small fraction of the total phase space in nearly-axisymmetric models.) Many workers have noted the “triaxial” nature of the orbit populations in nearly-prolate models.

Figures 3 and 4 illustrate the two initial condition spaces at shell 10 for 12 of the mass models. Regular orbits were assigned to one of three families: long-axis tubes, short-axis tubes and boxes. Long-axis tubes have a nonzero averaged angular momentum about the  $x$ -axis, short-axis tubes have a definite  $L_z$ , and boxes have no obvious, time-averaged angular momentum components.

The starting points of the three most important resonant orbit families are also plotted in Figures 3 and 4. The 1:1 orbits in the  $x - y$  plane generate most of the short-axis tubes; the 1:1 orbits in the  $y - z$  plane generate the long-axis tubes; and the 1 : 2  $x - z$  “banana” orbits generate many of the regular boxlike orbits. As found by Schwarzschild (1993), the number of minor resonances that generate regular orbits in the stationary initial condition space increases as the model becomes rounder.

### 4. Self-Consistent Models

The fraction of time spent by each orbit in a grid of cells was recorded, and a linear superposition of orbits was sought, with non-negative occupation numbers, that reproduced the known mass of the model in each cell. The details of the solution grid and of the optimization routine are given in Paper I.

When the full set of 6840 orbits was supplied to the optimization routine, self-consistent solutions were found for almost all of the 25 mass models. However, as discussed in Paper

I, such solutions are not bona-fide equilibria, since the optimization routine is free to assign arbitrary occupation numbers to the different stochastic orbits at each energy. In a real galaxy, chaotic mixing would tend to produce a uniform population of stochastic phase space at each energy on a timescale of order  $10^2$  dynamical times (Merritt & Valluri 1996). Thus, these quasi-equilibrium solutions would be expected to slowly evolve.

Fully stationary models can be constructed in one of two ways: by eliminating the stochastic orbits from the orbit libraries; or by replacing the set of stochastic orbits at each energy by an invariant ensemble representing a uniform population of stochastic phase space. The latter procedure was implemented in Paper I, where it was found that the inclusion of invariant ensembles reduced slightly the the residuals of the best-fit orbit population below those of a solution containing regular orbits alone. Here, the simpler alternative of omitting the stochastic orbits was chosen. This choice is not meant to suggest that nature would avoid placing stars on stochastic orbits in a real galaxy. However the invariant ensembles – because of their generally spherical shapes – are only a minor asset from the point of view of reconstructing the triaxial figure, and by omitting them one is likely to restrict only slightly the range of shapes that can be reproduced in a fully stationary way.

(This argument would be much less valid if applied to triaxial models with weak cusps or cores, in which the chaotic mixing timescales can be much longer (Goodman & Schwarzschild 1981; Merritt & Valluri 1996; Paper I). In such systems, a highly nonuniform population of stochastic phase space could presumably be maintained for a long period of time – in effect, many different stochastic orbits would exist at the same energy, giving much more freedom to construct a self-consistent equilibrium. Imposing secure limits on the degree of triaxiality would be difficult for such models since the range of allowable orbital populations would depend strongly on the degree to which stochastic phase space was assumed to be mixed. Most of this mixing presumably takes place during galaxy formation and so a solution to the self-consistency problem would require some knowledge about the formation process.)

Mass models for which self-consistent solutions containing only regular orbits were found are delineated in Figure 1. Only nearly axisymmetric, or spherical, mass models could be reconstructed from the regular orbits alone. Roughly speaking, models with  $T \lesssim 0.4$ ,  $T \gtrsim 0.9$  or  $c/a \gtrsim 0.8$  were found to have such solutions; the range in allowed values of  $T$  decreases with decreasing  $c/a$ , and no solutions containing just regular orbits were found for  $c/a = 0.4$ .

The fraction of the mass which these solutions place on the three orbit families are indicated in Figure 5. Bold-faced numbers refer to models for which self-consistency was

achieved; in the other models, the mass fractions shown in Figure 5 are those corresponding to the orbital population that most nearly reproduced the mass of the model in the cells. The variation found here in the orbital populations over the  $(c/a, T)$  plane may be compared to that found by Statler (1987, Fig. 6) in his study of fully integrable triaxial models. Nearly oblate (prolate), self-consistent models were found to contain a preponderance of short (long) axis tubes, similar to the results of Statler, and consistent with the expected form of the solutions in the axisymmetric limits. However the fraction of box orbits was found to be small,  $\lesssim 20\%$ , in all of the self-consistent solutions found here, even the substantially triaxial ones. By contrast, Statler found a much larger mass fraction in boxes, typically between 50% and 75% in models with  $c/a \lesssim 0.6$ . This difference is presumably due to the much narrower range of regular box orbit shapes in the potentials considered here, which makes them less useful for reproducing the figure. The largest box-orbit fractions found here were in models for which self-consistency could not be achieved; however even in these failed solutions the box orbit fraction never exceeded 40%.

Statler (1987) stressed the non-uniqueness of his solutions, i.e. the considerable freedom which he found to shift stars from one orbit family to another without violating self-consistency. One would expect much less degeneracy in our solutions, especially those lying near the curve in Figure 1 that divides allowed shapes from forbidden ones. Along this curve, which delineates the edge of solution space, the orbital populations are probably unique. The degree of non-uniqueness is likely to increase toward the oblate and prolate axes, since axisymmetric models are known to be degenerate in their orbital populations (e.g. Dehnen & Gerhard 1993). However no attempt was made here to explore the degree of degeneracy of the solutions.

## 5. Discussion

A long-standing puzzle in the study of elliptical galaxies is the narrow range of morphological and kinematical properties which they exhibit. Kinematical tests for non-axisymmetry in well-selected samples find little evidence for strong triaxiality; most ellipticals appear to be either nearly oblate or nearly prolate (Franx, Illingworth & de Zeeuw 1991). Detailed studies of the velocity fields of individual galaxies also imply that axisymmetry is the norm, at least in galaxies where the stellar distribution is likely to be relaxed (Statler 1994; Qian et al. 1995; Statler, Smecker-Hane & Cecil 1996). Among elliptical galaxies of a given luminosity, the distribution of Hubble types is quite narrow. Bright ellipticals have an apparent shape distribution that is peaked at  $b/a \approx 0.85$  with a dispersion of only  $\sim 0.1$  (Ryden, Lauer & Postman 1993). This distribution is

inconsistent with complete axisymmetry but only mildly so (Tremblay & Merritt 1996). The Hubble-type distribution of fainter ellipticals is not so well determined but is also fairly narrow; the peak lies at an apparent axis ratio of  $\sim 0.7$  and the distribution is fully consistent with axisymmetry (Tremblay & Merritt 1996).

In their kinematics, too, elliptical galaxies show surprisingly little variation. The line-of-sight velocity distributions, whose shapes reflect to some degree the average character of the stellar orbits, are almost always nearly Gaussian. The most prominent deviations are asymmetric ones resulting from the rotation of a distinct subcomponent (e.g. Franx & Illingworth 1988); large symmetric deviations – like those expected in spherical models with strong velocity anisotropy, for instance – are almost never observed (Bender, Saglia & Gerhard 1994). Together with the virial theorem, this homogeneity in the shapes and kinematics of elliptical galaxies implies that their observable scaling parameters (diameter, velocity dispersion, surface brightness) should be tightly correlated. This is in fact the case: elliptical galaxies define a “Fundamental Plane” which is extremely thin (Djorgovski & Davis 1987).

Until recently, theoretical work provided little in the way of explanation for this homogeneity. Studies of the axisymmetric and triaxial self-consistency problems (mostly in the context of mass models with large cores) demonstrated again and again the extremely wide range of possible solutions, both morphological and kinematical (Statler 1987; Dehnen & Gerhard 1993; Hunter 1995). Stability studies, while ruling out some models extreme in their shapes (e.g. Merritt & Sellwood 1994) or kinematics (e.g. Saha 1991), failed to narrow this range appreciably.  $N$ -body simulations of elliptical galaxy formation also tended to generate models with a much wider range of properties than observed. The shapes and kinematics of galaxies produced by the merger of  $N$ -body disks, for instance, are strongly correlated with the relative orientation of the colliding galaxies (Barnes 1992). These  $N$ -body remnants are often highly flattened, triaxial, or box-shaped, in sharp contrast with the majority of observed ellipticals. Dark halos produced in simulations of hierarchical structure formation tend to be highly elongated and triaxial (Warren et al. 1992), again quite unlike real elliptical galaxies.

We propose here that the narrow range of elliptical galaxy shapes and kinematics may be a simple consequence of dynamical self-consistency. We consider first faint ellipticals, which have stellar density cusps that are predictably as steep as  $r^{-2}$ . Figure 1 shows that stationary models with strong cusps are very limited in their allowed shapes: they must be nearly oblate ( $T \lesssim 0.4$ ), nearly prolate ( $T \gtrsim 0.9$ ), or nearly spherical ( $c/a \gtrsim 0.8$ ). Given the narrowness of the allowed region along the prolate boundary in Figure 1, we might further expect oblate and spherical shapes to be preferred over prolate ones. These predictions are

consistent with what little is known about the intrinsic shapes of low-luminosity elliptical galaxies. The flattenings of faint ellipticals correlate with their rotation in the manner expected for “oblate isotropic rotators” (Davies et al. 1983), circumstantial evidence that they are approximately oblate. Axisymmetry is also consistent with the frequency function of Hubble types of faint ellipticals, but the same is true of a triaxial shape distribution (Tremblay & Merritt 1996). Detailed modelling of two-dimensional velocity fields has now been carried out for a few galaxies; among these, M32 is faint,  $M_V = -16.3$ , and appears to be accurately oblate (Qian et al. 1995).

Our results might also predict a narrow range of *kinematical* properties for galaxies with strong cusps. Suppose that nature constructed a galaxy with a strong cusp and with an initial shape that placed it outside of the region corresponding to self-consistent solutions in Figure 1. Such a galaxy would not be able to reach an equilibrium state without changing its shape. Although the direction of that change is not obvious, the galaxy would eventually cross the curve that separates allowed from forbidden shapes in Figure 1. Since the orbital population of an equilibrium model near this curve is likely to be unique – as argued above – one would expect galaxies so produced to have kinematical properties that are strongly correlated with their shapes.

(The orbital compositions of real galaxies produced in this way would probably differ somewhat from those of the models constructed here, since nature would not exclude stars from the stochastic parts of phase space. However the mass fractions associated with stochastic orbits in fully stationary galaxies are likely to be modest (Paper I).)

The results presented here are not so clear in their implications for bright elliptical galaxies,  $M_V \lesssim -20.5$ , which exhibit a range of cusp density slopes (Merritt & Fridman 1995). Chaotic mixing timescales of boxlike orbits can be quite long when the cusp is weak or nonexistent (Goodman & Schwarzschild 1981; Merritt & Valluri 1996), implying more freedom to reconstruct a triaxial shape. However many elliptical galaxies, both bright and faint, may contain massive nuclear black holes like those in M32 and M87 (Kormendy & Richstone 1995); in fact it has been suggested that the weak stellar cusps of bright ellipticals are produced during the coalescence of two black holes following a merger (Ebisuzaki, Makino & Okumura 1991). The properties of stochastic orbits in triaxial potentials with massive central singularities are similar to those in triaxial potentials with strong cusps (Merritt & Valluri 1996). If massive nuclear black holes are ubiquitous, we might expect bright ellipticals to also be strongly constrained in their shapes. Interestingly, the Hubble-type distribution of elliptical galaxies with  $M_V \lesssim -20.5$  is strikingly different from that of fainter ellipticals and appears to require a certain number of non-axisymmetric galaxies (Tremblay & Merritt 1996). The sample of (mostly bright) ellipticals analyzed by

Franx, Illingworth & de Zeeuw (1991) also contains a few members with significant minor axis rotation, hence probably triaxial. But these facts are not obviously inconsistent with Figure 1, since strongly triaxial shapes are permitted when  $c/a \gtrsim 0.8$ . A large fraction of bright elliptical galaxies satisfy this condition (Tremblay & Merritt 1996).

Many of the systematic differences between bright and faint ellipticals – including the steepness of the cusps – are thought to result from the greater importance of gaseous dissipation during the formation of the latter (Faber et al. 1997). Are the purely stellar-dynamical arguments presented here relevant to galaxies that formed dissipatively? Barnes (1996) has discussed how the addition of a dissipative component to  $N$ -body simulations of disk galaxy mergers can affect the final shape and kinematics of the remnant. In the absence of gas, the remnants are often strongly triaxial, containing many stars on box orbits. When gas is included, gravitational torques during the merger deposit much of the gas near the center on a short timescale, deepening the potential well there. The stellar component of the galaxy responds by becoming more oblate. Barnes & Hernquist (1996) speculate that this change in shape is driven by the destabilization of box orbits which pass near the center – the same mechanism that is responsible for ruling out strongly triaxial models in the present study. A number of authors have noted similar changes in the shape of an initially triaxial,  $N$ -body galaxy following an increase in the central density (e.g. Norman, May & van Albada 1985; Udry 1993; Dubinski 1993). The dissipative formation of galaxies is undoubtedly complex, but these arguments suggest that the evolution toward more oblate shapes seen in numerical simulations with dissipation can be explained in part by the absence of strongly triaxial equilibria.

## 6. Summary

Strong triaxiality is inconsistent with a high central density. Dynamical models with Jaffe’s density law, which has  $\rho \propto r^{-2}$  near the center, must be nearly oblate ( $T = (a^2 - b^2)/(a^2 - c^2) \lesssim 0.4$ ), nearly prolate ( $T \gtrsim 0.9$ ) or nearly spherical ( $c/a \gtrsim 0.8$ ). This result may explain in part the homogeneity of elliptical galaxies, including the tendency of low-luminosity ellipticals to be oblate, and the narrow range of elliptical galaxy kinematical properties.

This work was supported by NSF grant AST 90-16515 and by NASA grant NAG 5-2803. G. Quinlan’s assistance in the programming is gratefully acknowledged. T. Fridman and M. Valluri kindly read a first draft and made useful suggestions for changes.

## REFERENCES

Barnes, J. E. 1992, ApJ, 393, 484

Barnes, J. E. 1996, in The Formation of Galaxies, Proceedings of the V Canary Islands Winter School of Astrophysics, ed. C. Muñoz-Tuñón (Cambridge: CUP)

Barnes, J. E. & Hernquist, L. 1996, ApJ, 471, 115

Bender, R., Saglia, R. P. & Gerhard, O. E. 1994, MNRAS, 269, 785

Davies, R. L., Efstathiou, G., Fall, S. M., Illingworth, G. & Schechter, P. L. 1983, ApJ, 266, 41

Dehnen, W. & Gerhard, O. E. 1993, MNRAS, 261, 311

de Zeeuw, P. T. & Lynden-Bell, D. 1985, MNRAS, 215, 713

Djorgovski, S. & Davis, M. 1987, ApJ, 313, 59

Dubinski, J. 1993, ApJ, 431, 617

Ebisuzaki, T., Makino, J. & Okumura, S. K. 1991, Nature, 354, 212

Faber, S. et al. 1997, preprint

Fasano, G. & Bonoli, C. 1989, A&AS, 79, 291

Franx, M., Illingworth, G. & de Zeeuw, T. 1991, ApJ, 383, 112

Franx, M. & Illingworth, G. 1988, ApJ L, 327, L55

Gebhardt, K. et al. 1996, AJ, 112, 105

Goodman, J. & Schwarzschild, M. 1981, ApJ, 245, 1087

Hui, X., Ford, H. C., Freeman, K. C. & Dopita, M. A. 1995, ApJ, 449, 592

Hunter, C. 1995, Ann NY Acad Sci, 751, 76

Jaffe, W. 1983, MNRAS, 202, 995

Kandrup, H. E. & Mahon, M. E. 1994, Phys. Rev. E, 49, 3735

Kandrup, H. E. & Mahon, M. E. 1995, Ann NY Acad Sci, 751, 93

Kormendy, J. & Richstone, D. O. 1995, ARA&A, 33, 581

Kuzmin, G. G. 1973, in The Dynamics of Galaxies and Star Clusters, ed. T. B. Omarov (Nauka of the Kazakh S. S. R., Alma-Ata), 71.

Longo, G., Zaggia, S. R., Busarello, G. & Richter, G. 1994, A&AS, 105, 433

Merrifield, M. & Kuijken, K. 1992, ApJ, 432, 575

Merritt, D. 1980, ApJ S, 43, 435

Merritt, D. & Fridman, T. 1995, A. S. P. Conf. Ser. Vol. 86, Fresh Views of Elliptical Galaxies, ed. A. Buzzoni, A. Renzini & A. Serrano (Provo: Astronomical Society of the Pacific), 13

Merritt, D. & Fridman, T. 1996, ApJ, 460, 136 (Paper I)

Merritt, D. & Sellwood, J. A. 1994, ApJ, 425, 551

Merritt, D. & Valluri, M. 1996, ApJ, 471, 82

Möllenhoff, C. & Bender, R. 1989, A&A, 214, 61

Nieto, J.-L., Bender, R., Poulain, P. & Surma, P. 1992, A&A, 257, 97

Norman, C., May, A. & van Albada, T. 1985, ApJ, 296, 20

Papaphilippou, Y. & Laskar, J. 1997, preprint

Qian, E. E., de Zeeuw, P. T., van der Marel, R. P. & Hunter, C. 1995, MNRAS, 274, 602

Rubin, V. C., Graham, J. A. & Kenney, J. D. P. 1992, ApJ, 394, L9

Ryden, B. S., Lauer, T. R. & Postman, M. 1993, ApJ 410, 515

Saha, P. 1991, MNRAS, 248, 494

Schwarzschild, M. 1979, ApJ, 232, 236

Schwarzschild, M. 1982, ApJ, 263, 599

Schwarzschild, M. 1993, ApJ, 409, 563

Statler, T. S. 1987, ApJ, 321, 113

Statler, T. S. 1994, AJ, 108, 111

Statler, T., Smecker-Hane, T. & Cecil, G. N. 1996, AJ, 111, 1512

Tremblay, B. & Merritt, D. 1996, AJ, 111, 2243

Udry, S. 1993, A& A, 268, 35

Warren, M. S., Quinn, P. J., Salmon, J. K. & Zurek, W. H. 1992, ApJ, 399, 405

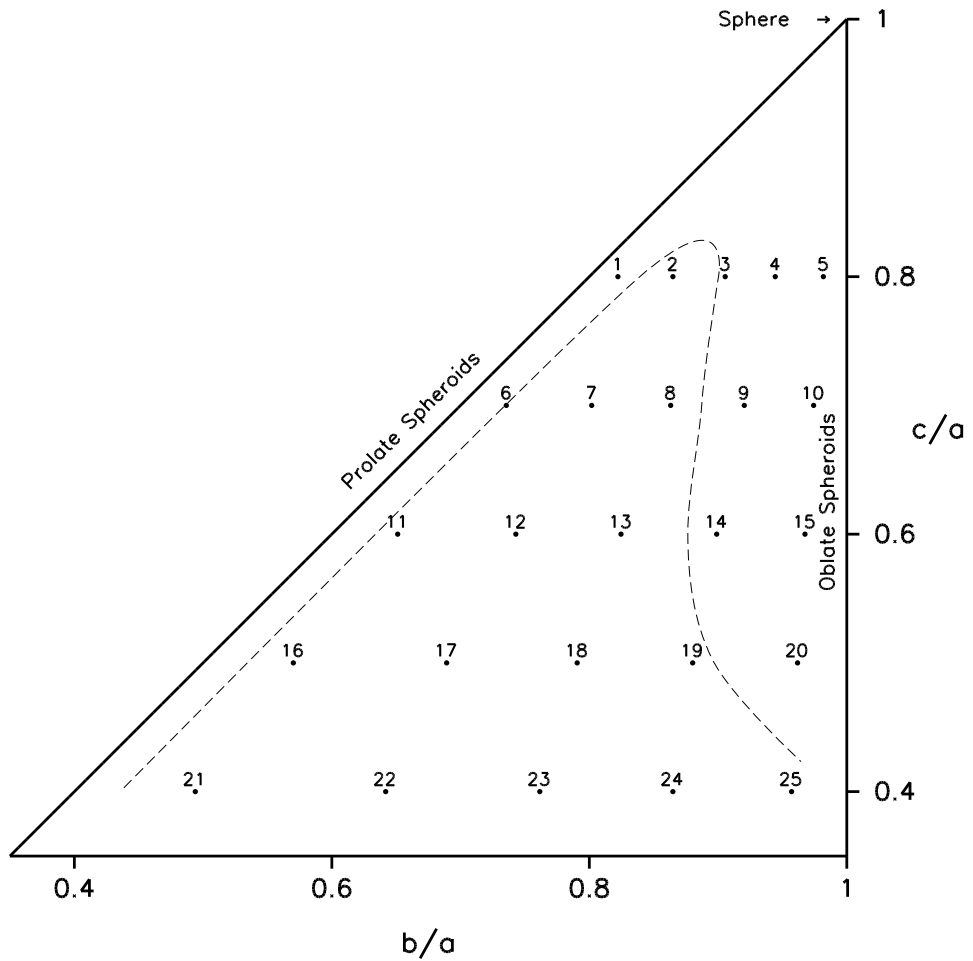


Fig. 1.— Plane of axis ratios, showing the 25 models of the survey. The dotted curve denotes the approximate limit of solution space; points below correspond to models for which no self-consistent solution was found.

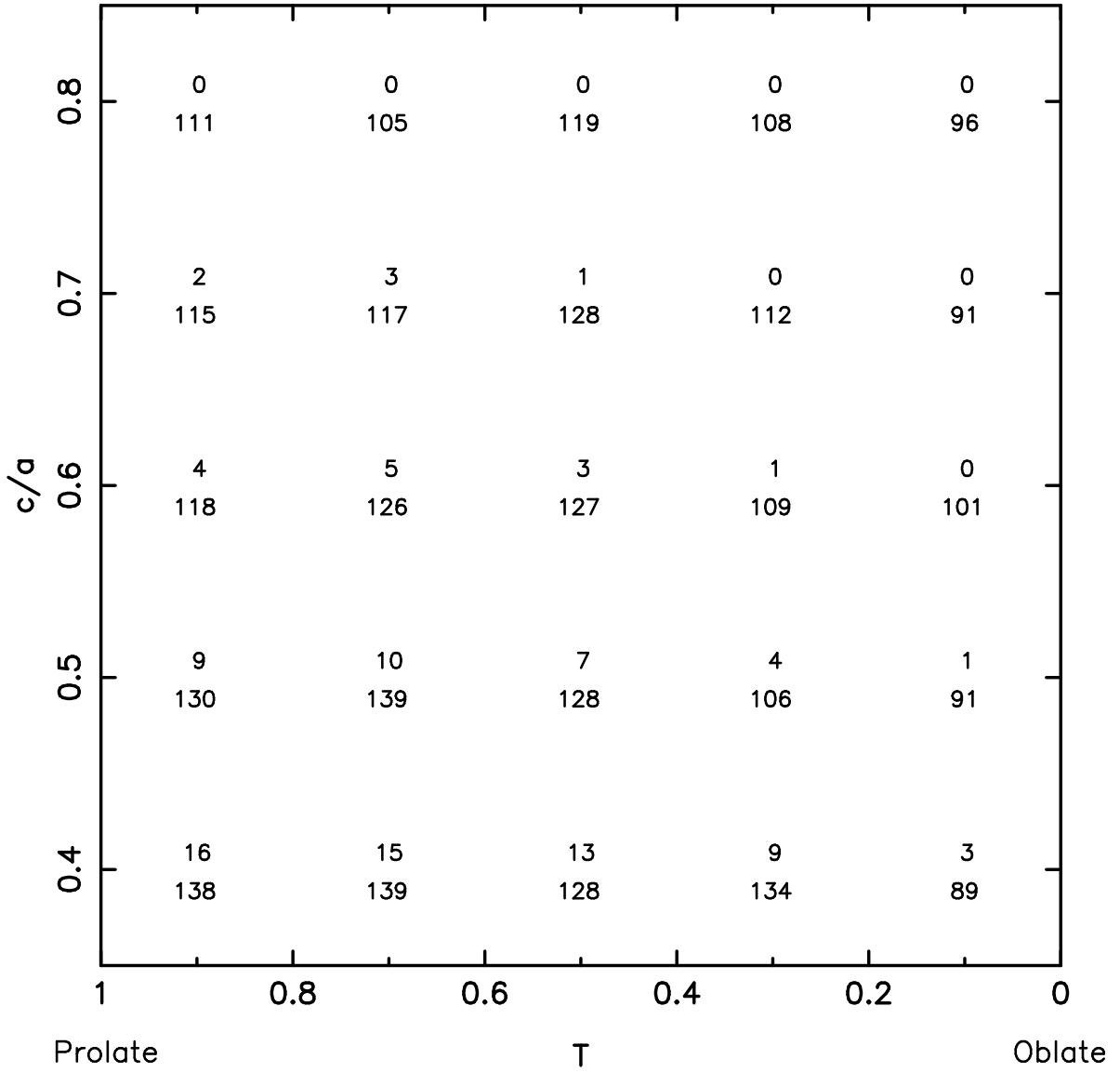


Fig. 2.— Average number of stochastic orbits per shell in the 25 models, out of a total of 150 ( $x - z$  initial condition space; top numbers) or 192 (stationary initial condition space; bottom numbers).

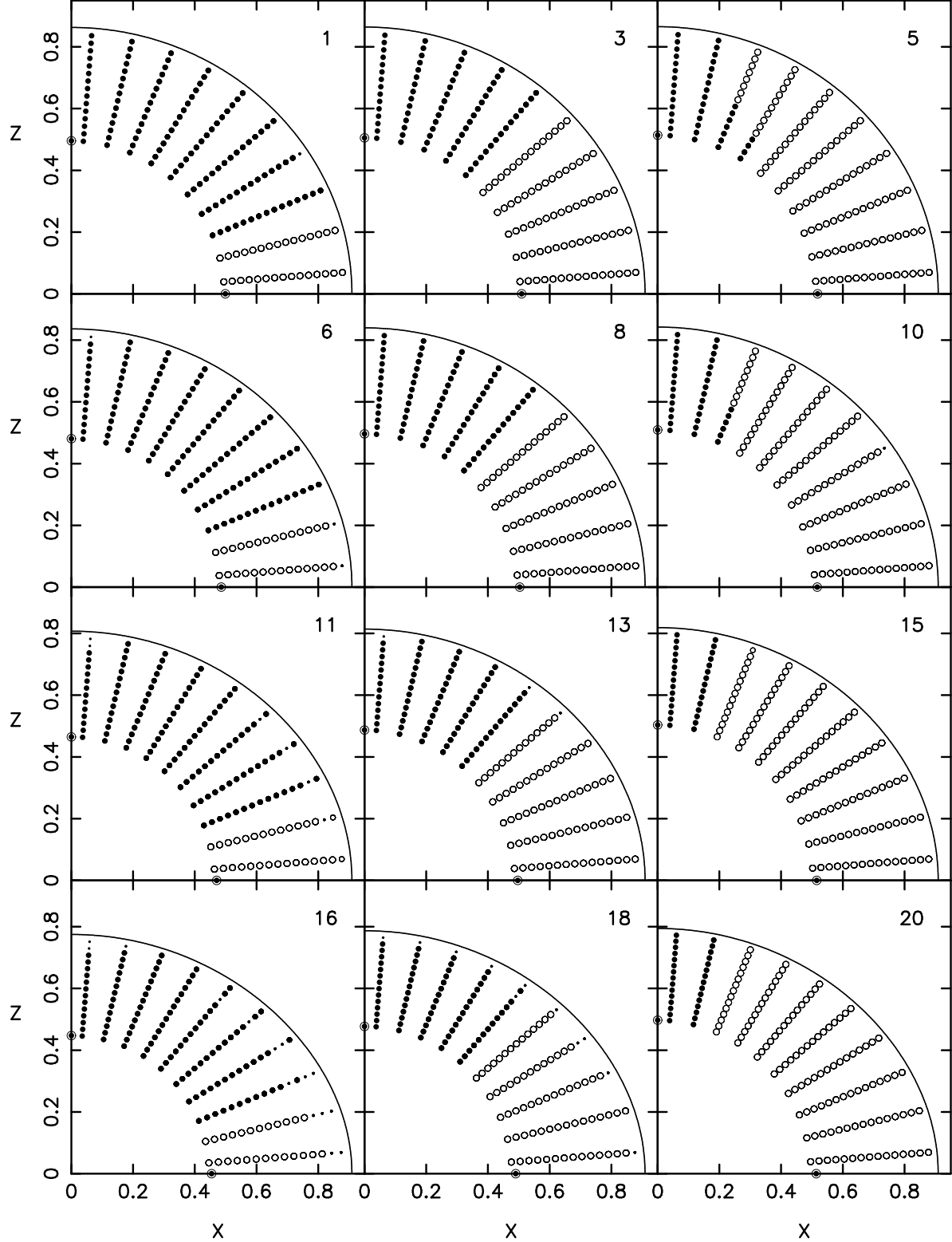


Fig. 3.—  $x - z$  initial condition space at shell 10 for a set of models. Numbers in the upper right of each frame correspond to positions in the axis-ratio plane of Figure 1. Filled circles denote the long-axis tubes, large open circles the short-axis tubes, small open circles the boxes, and small dots the stochastic orbits. Circled dots are the 1:1 resonant orbits in the  $x - y$  and  $y - z$  planes.

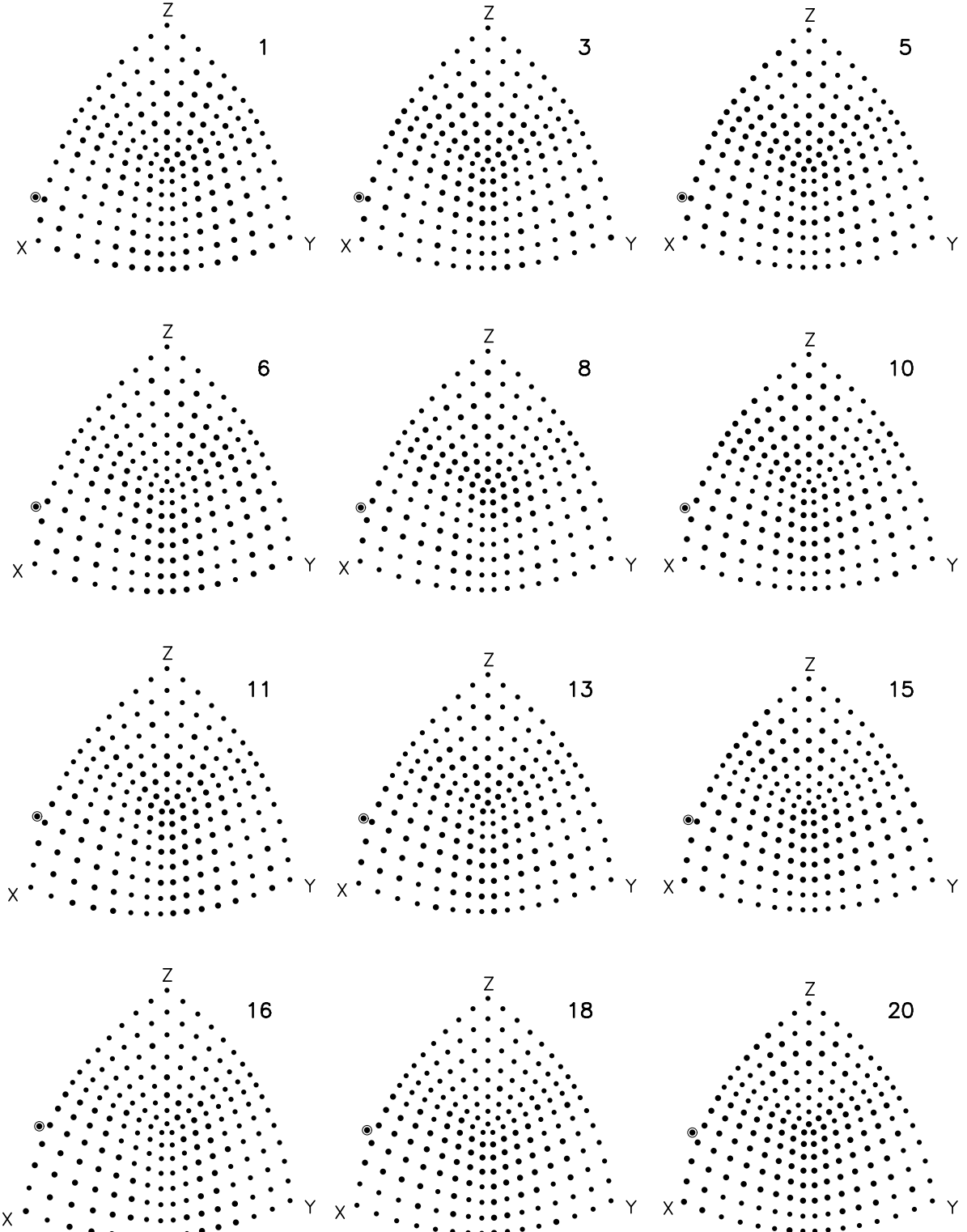


Fig. 4.— Stationary initial condition space at shell 10 for a set of models. Numbers in the upper right of each frame correspond to the positions in the axis-ratio plane of Figure 1. Large dots denote the regular orbits and small dots the stochastic orbits. Circled dots are the 1:2 resonant “banana” orbits in the  $x - z$  plane.

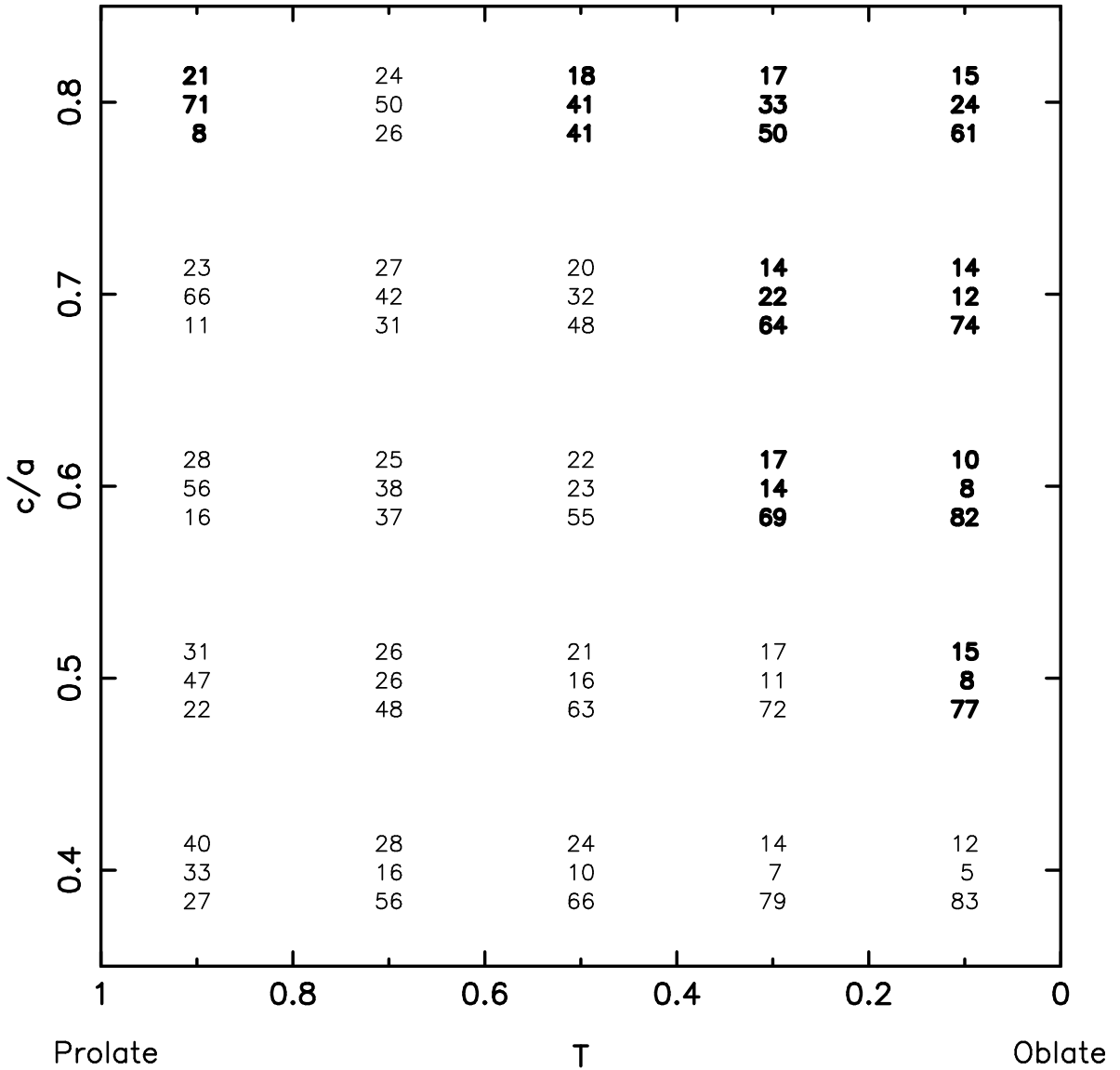


Fig. 5.— Orbital mass fractions for the numerical solutions. The top number indicates the percentage of the total mass in box orbits, the middle number the percentage in long-axis tubes, and the lower number the percentage in short-axis tubes. Bold-faced numbers refer to models for which self-consistency was achieved.